

RF DESIGN OF THE POWER COUPLER FOR THE SPIRAL2 SINGLE BUNCH SELECTOR*

F. Consoli, A. Caruso, G. Gallo, D. Rifuggiato, E. Zappalà, INFN-LNS, Catania, Italy
M. Di Giacomo[#], GANIL-SPIRAL2, Caen, France

Abstract

The single bunch selector of the Spiral2 driver uses high impedance travelling wave electrodes driven by fast pulse generators. The characteristic impedance of 100 Ohm has been chosen to reduce the total power, but this non standard value requires the development of custom feed-through and transitions to connect the pulse generators and the matching load to the electrodes. The paper reviews the design of these devices.

INTRODUCTION

The single-bunch selector of the Spiral2 accelerator reduces the bunch repetition rate onto the experimental target of a factor 100 to 10000. The device is constituted of a static magnetic deflector and of a pulsed RF kicker whose fields are perfectly compensated for the selected bunch. All other bunches are deviated onto a beam stop by the magnetic field. This principle, shown in Fig. 1, inverts the duty cycle required for the RF kicker and uses constant length pulses.

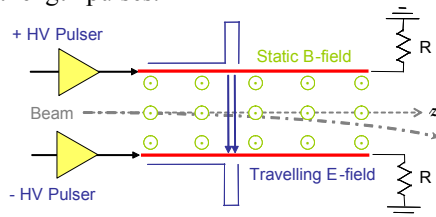


Figure 1: Principle of the inverted duty cycle single bunch selector.

This solution was developed in the framework of the Eurisol Design Study [1] and is justified by the high repetition rate, high voltage, and fast transient time required by high intensity ion drivers. Table 1 reports the values for the Spiral2 application.

Table 1: Single Bunch Selector Requirements

Parameter	Value	Units
Repetition rate	1	MHz
Rise and fall time	6	ns
Pulse total length	19	ns
Pulse max voltage	2.5	kV
Pulsers power	1	kW

Table 2 gives the operating parameters for a plate length of 546 mm and for the different kinds of ions

*Work supported by the European Community FP7 – Capacities – SPIRAL2 Preparatory Phase n° 212692.

[#]digiaco@ganil.fr

(identified by their mass to charge ratio A/q) of the Spiral2 driver. The difference between the beam and the plate voltages is due to the coverage factor of the meander plate, which is ~ 0.75 .

Table 2: Voltage Requirements for the SBS

A/q	Beam Voltage	Pulse Voltage
1	473 V	630 V
2	792 V	1056 V
3	1182 V	1576 V
6	1773 V	2364 V

High voltage switches being too slow and not enough powerful, the travelling wave solution was proposed in the inverted duty cycle configuration in order to reduce the involved RF power.

The electromagnetic field of the RF kicker is generated by two pulsers of opposite sign travelling along two meander-shaped microstrips ($\beta 0.04$), each one ended by a matching load.

Characteristic impedance (Z_c) of 100 Ohm has been chosen as a compromise among pulser RF power, meander loss, and meander feasibility.

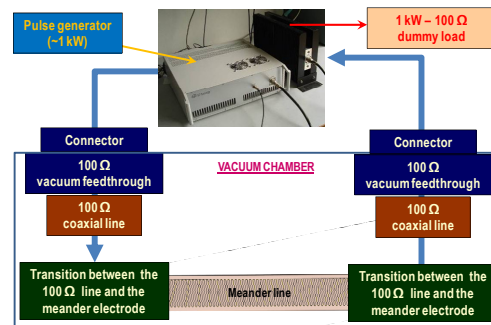


Figure 2: Schematics of the meander feeding chains.

As shown in Fig. 2, the signal of each generator is transmitted via 100 Ohm cables supplied by the pulser manufacturer. From the cable, the pulse travels through the feed-through, where the vacuum window is located, and a short section of transmission line before reaching the transition to the meander strip. A similar path is followed at the output to reach the matching load.

All the feeding chain elements have been designed to minimize the insertion and transition loss to transfer the best possible pulse. CST Microwave Studio was used for RF simulation in both time and frequency domains and results of the different simulations are reported here. An

analysis bandwidth of 150 MHz has been considered for the pulse spectrum.

POWER COUPLER

Feed-Through and Connector

The feed-through and the connection to the 100 Ohm cable are strictly related. Three cases have been studied: two custom 100 Ohm devices, using cylindrical (a) and disk (b) vacuum windows as shown in Fig. 3 and a set of HN 50 Ohm standard cable and feed-through connectors.

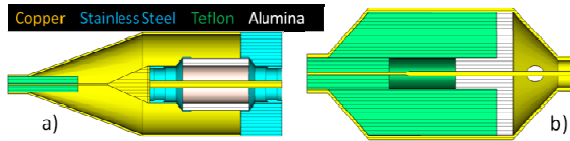


Figure 3: Simulated 100 Ohm feed-throughs. Scale of geometry a) is almost twice smaller than that of case b).

Solution (a) has been studied first but rapidly abandoned because it requires more room than the one with the disk break (b), which has been studied more in details. The inner conductor connection between the cable and the feed-through is to be brazed to avoid complicate machining. The maximum electric field at this point is ~2 MV/m, lower than the air dielectric strength value, considered of 3 MV/m. Consequently, a Teflon shell is introduced between the two conductors to reduce the sparking risk. In fact, the disc Alumina is T-shaped so that the Teflon can be superposed to the ceramic, as it is done in HV standard connectors. The ground connection is granted by tight mechanical contact. On the vacuum side, the diameter ratio changes to $Z_c = 100$ Ohm. The inner conductor diameter is chosen of 1.2 mm, as beyond this value it is more difficult to braze the Alumina, and the resulting outer diameter is 6.4 mm. The corresponding electric field is ~2 MV/m, well below the vacuum dielectric strength value.

To simulate the set of standard HN devices, some approximations in the modelling had to be introduced, since it hasn't been possible to have precise information from the data sheets. Only Teflon has been considered as dielectric, and probably the feed-through behaviour would be worse due to the higher dielectric constant of the Alumina, used for the vacuum window. The simulated geometry includes the section where the cable is inserted, which has characteristic impedance higher than 100 Ohm, and the section before the short transition to the 100 Ohm line on the vacuum side, where Z_c is ~60 Ohm. Lengths of each section are shown in Fig. 4.

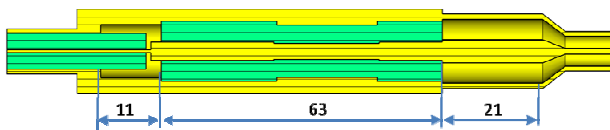


Figure 4: HN simulated structure with 100 Ohm cable (left size) and ending transition to 100 Ohm (right size).

Comparative results for the S parameters and for the pulse deformation are shown in Fig. 5, where (c) indicates the

50 Ohm geometry. The input pulse is approximated with the function:

$$s(t) = \begin{cases} 2500 \cdot \frac{1 - \cos\left(\frac{\pi t}{2 \cdot 10^{-9}}\right)}{2} & 0 \leq t \leq 6 \cdot 10^{-9} \\ 2500 & 6 \cdot 10^{-9} \leq t \leq 13 \cdot 10^{-9} \\ 2500 \cdot \frac{1 - \cos\left[\pi \left(1 - \frac{t - 13 \cdot 10^{-9}}{6 \cdot 10^{-9}}\right)\right]}{2} & 13 \cdot 10^{-9} \leq t \leq 19 \cdot 10^{-9} \end{cases} \quad (1)$$

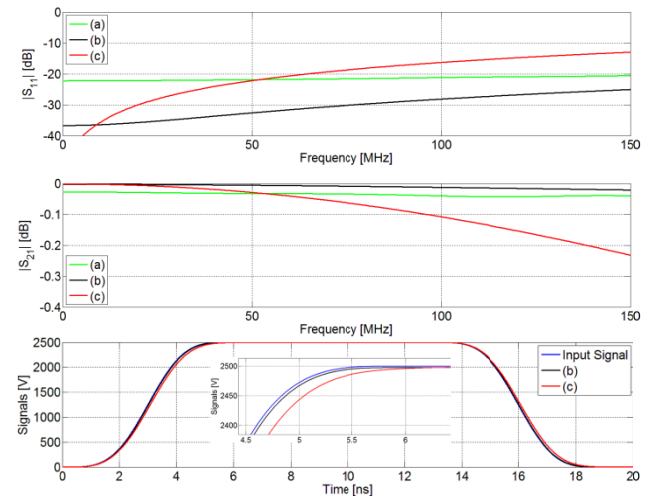


Figure 5: S parameters for the (a) and (b) 100 Ohm feed-throughs of Fig. 3 and for the HN 50 Ohm structure (c) of Fig. 4. Time domain results for the (b) and (c) cases.

100 Ohm Coaxial Line

Between the feed-through and the meander transition, a 100 Ohm coaxial line is inserted. The outer coaxial is equipped with longitudinal slots for proper vacuum pumping inside the volume concerned by the RF fields. The slots do not change significantly insertion and transmission loss, as shown in Fig. 6.

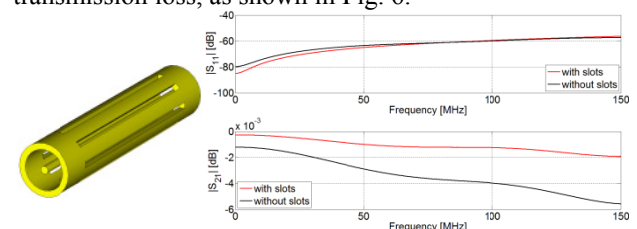


Figure 6: Slotted coaxial line and S parameters.

The ground connection is granted by tight contact, while the inner conductor is part of the feed-through and the tip ends onto a pad of the meander strip.

Coupler Mechanics

To avoid the presence of internal spacers, a straight section of line is used as shown in Fig. 7. Consequently the coupler has to face the transition collar.



Figure 7: Feed-through and 100 Ohm slotted line.

TRANSITION TO THE MEANDER STRIP

Both longitudinal and perpendicular solutions have been investigated for the transition between the coaxial line and the 100 Ohm microstrip. Results of Fig. 8 show similar behaviour, with negligible effect on the pulse shape.

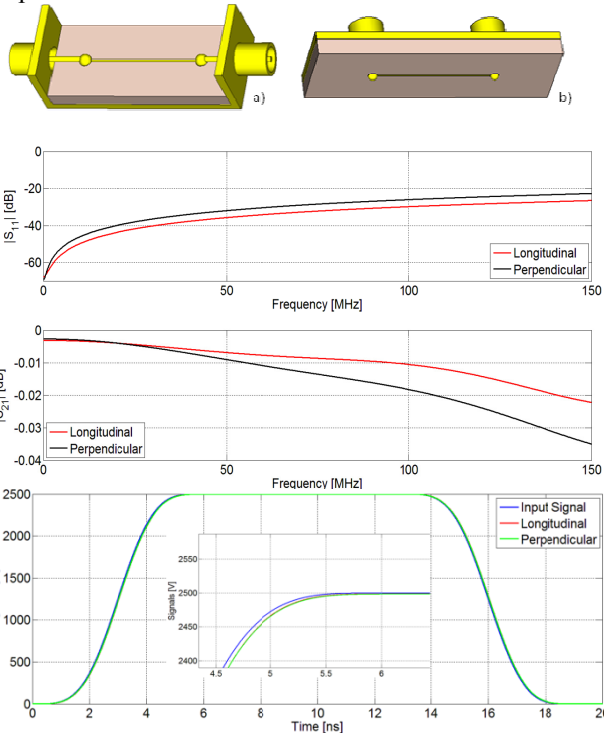


Figure 8: Longitudinal (a) and perpendicular (b) geometries and comparison of their S parameters and pulse responses.

As a 1 kW pulse has to be transferred, we consider that the contact to the strip has to be brazed. In this way we also grant the cooling of the coaxial line wire via the Alumina. Brazing on the microstrip is possible by warming the plate up to some 45°C by driving it with 5 or 6 A of DC current.

All the previous simulations show the effect of the different elements of the coupler. To compare these results to the pulse deformation due to the electrode itself, the perpendicular transition has been used with the whole 78-periods meander shown in Fig. 9.

CONCLUSIONS

Different solutions have been studied for the power coupler of the single bunch selector meander line and for the transition to the microstrip. The most critical element is the feed-through, the meander transition and the slotted coaxial line having very low effect on the pulse deformation. The coupler designed with the custom feed-through based on a disk vacuum window gives the best results, as the transient times are slowed down of few tens of nanoseconds only. Acceptable results could in principle be achieved with the HN set too. We can conclude that the effect of the designed coupler is negligible with respect to the pulse deformation due to the

length, the attenuation and the frequency dependent delay of the meander line. Manufacturing and assembling issues have been studied too and a prototype including a vacuum chamber, two water cooled electrode holders and four couplers is being designed at INFN-LNS. Power tests will quantify maximum performances of the proposed solution.

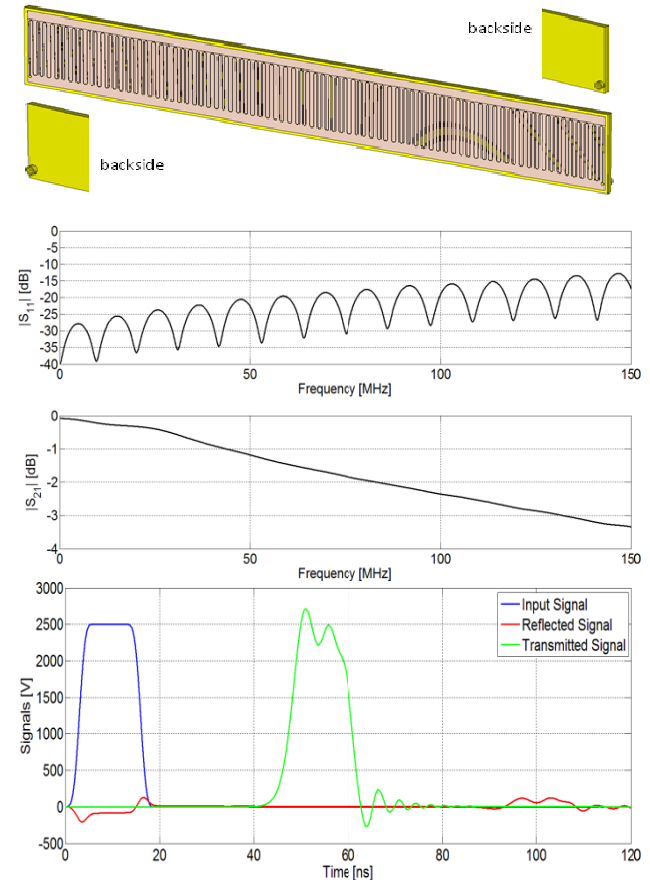


Figure 9: Pulse deformation due to the 78-period meander line fed by the perpendicular transitions.

ACKNOWLEDGEMENT

The authors are grateful to P. Balleyguier (CEA/DAM) who reviewed the design work and suggested to use equation (1) for the input signal, in order to get more realistic simulations.

REFERENCES

- [1] G. Le Dem, M. Di Giacomo: "A Single Bunch Selector for the next low β continuous wave heavy ion beam", PAC'07, Albuquerque, New Mexico, USA, 25-29 June 2007, MOPAN008, p. 158 (2007); <http://www.JACoW.org>.
- [2] P. Balleyguier, M. Di Giacomo, M. Michel, G. Fremont, P. Bertrand: "Electrode Design Improvement in the SPIRAL2 Single Bunch Selector", LINAC2010, Tsukuba, Japan, 12-17 September 2010.